United Nations Educational, Scientific and Cultural Organization
Geothermal Training Programme Under the auspices of UNESCO

GRÓ GTP, Grensásvegur 9,
IS-108 Reykjavík, Iceland

Reports 2021
Number 9

ELECTRICITY GENERATION FROM HIGH WATER CUT OIL AND GAS WELLS BY COMBINED GEOTHERMAL ORC AND GAS TURBINE SYSTEM

Mohamad Hasan Javadi
Geothermal group – Niroo Research Institute (NRI)
End of Dadman blvd, Shahrak Ghods, Tehran
IRAN
moja@grogtp.is; mohamadhasan.javadi@yahoo.com

ABSTRACT

Geothermal energy is a clean energy form that has been developed significantly during recent decades and is seen as one of the solutions for fighting climate change. Developing geothermal resources from exploration to exploitation involves high cost and risk that limits the growth rate of geothermal energy utilization globally. Also, conventional geothermal projects are not feasible economically in oil and gas producing countries such as Iran, where low-cost fossil fuels are used to provide the required electricity and heat. Yet, there are thousands of wells, available infrastructure, and useful data (exploration and production history) in oil and gas fields. Finding ways to extract the available geothermal energy in these fields eliminates the high cost and risks of the exploration and drilling stages of geothermal projects, which constitute more than half of the total cost and risk. Also, there are deep and vast high-pressure water aquifers below hydrocarbon layers that are intersected by oil/gas production wells and remain at high pressure. Because the aquifers are located at depths of more than 1 km, they contain valuable geothermal energy. Co-producing large volumes of water in mature oil and gas fields is a typical problem for operation companies, which increases the cost and forces the operators to abandon high water cut wells (wells with a high water to total fluid production ratio). Since this water is produced from deep layers, it contains geothermal energy, which could be used for both direct and indirect applications. Commonly, geothermal resources in oil and gas fields are categorized as low to moderate temperature resources (temperature of less than 150°C) and they contain dissolved gas. The aim of this study is to explore the option of using the dissolved or free produced gas to generate electricity with a gas turbine and using the exhaust of this system to heat up warm co-produced water, which would then be used in an Organic Rankin Cycle (ORC) to produce green energy. In this study, CO_2 production per kWh and net power output of three different cases (only gas turbine and two combined systems with different natural gas flowrates) are compared to show the possibility and advantages of using the available geothermal energy in oil and gas fields. Results show that using the hot exhaust gas increases the power generation and makes geothermal water suitable for usage in an ORC power plant. Finally, we carry out a sensitivity analysis to study the impacts of parameters (co-produced water temperature, flowrate, and the ratio of dissolved gas) on system characteristics. The proposed results of this investigation could be used for further practical studies investigating the harnessing of geothermal energy in oil and gas fields.

1. INTRODUCTION

Geothermal energy is a type of the renewable energy which is stored in subsurface layers and its energy content increases with depth. Based on the geothermal resource temperature, they are classified as high (>150°C), intermediate (90-150°C) and low temperature (30-90°C) resources, which indicates the power and possible utilization applications (Chiasson, 2016). As opposed to other forms of energy (fossil fuels and renewables, solar, wind, etc.) geothermal power is available in every weather condition and geographical location doesn't restrict its advantages. Therefore, it has been developed intensively in recent decades to decrease greenhouse emissions and global warming effects. Predictions say that by a share of approximately 3.5% in 2050, geothermal energy will play an important role in the future of the global electricity generation mix (Haghighi et al., 2020).

Basically, geothermal utilization is divided into direct and indirect (electricity generation) methods which depend on the resource temperature. Although electricity generation by single and double flash power plants is well-known for high temperature resources which are commonly located near volcanoes (DiPippo, 2015), recently, organic Rankin cycles (ORC) have been used to generate power from lower temperature reservoirs which are more available globally and for which common power generation methods are not feasible options from an economical point of view (DiPippo, 2015; Ahmadi et al., 2020). Altogether, the installed capacity of geothermal power generation has increased by 3.65 GW_e between 2015 and 2020 to 16.0 GW_e and 95,100 GWh/year were produced in 2020 (Huttrer, 2020).

Also, direct utilization of geothermal power could be used for different applications such as space heating, food industry, agriculture, aquaculture, water desalination, etc. This has experienced noticeable growth of 52.0% between 2015 and 2019 (8.73 %/yr), bringing the installed capacity to 107 GW_{th}. According to data from late 2019, 1,020,000 TJ/yr (284,000 GWh_{th}/yr) of thermal energy were used which is a 72.3% rise compared to 2015 and indicates an annual growth rate of 11.5% (Lund and Toth, 2021).

Drilling wells (exploration, production and injection) is vital for the development of a geothermal project, and, as it is shown in Figure 1, it corresponds to more than half of the total cost of the project. The cost is also about two times higher for low temperature reservoirs (Clauser and Ewert, 2018). In addition to the higher costs of exploration and drilling, the operational risk during pre-construction stages is also much higher than during later stages (Gehringer and Loksha, 2012). Therefore, the high cost of drilling wells and risky processes of exploration has restricted the growth rate of geothermal energy use, compared to other types of renewable energies (Clauser and Ewert, 2018).

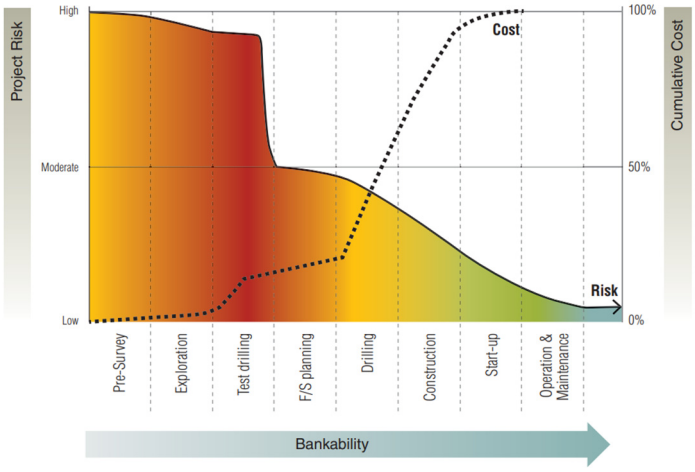

FIGURE 1: Costs and risks management during the different stages of geothermal project development (Gehringer and Loksha, 2012)

Conventional oil and gas reservoirs usually include deep aquifers with high pressure and temperature below the hydrocarbon layers, which drives oil and gas toward the production wells. Over time, production causes the reservoirs to become depleted, and an increasingly large amount of water is produced as a by-product, called "co-produced water". As well as the aquifers, unconventional reservoirs such as shale or coal reservoirs and production scenarios like water flooding, steam injection, hydraulic fracturing and other methods can affect both volume and quality of co-produced water at the surface (Nasiri et al., 2017).

This large volume of water has been known as waste for oil operation companies which makes reservoir management difficult and severely increases operational costs and finally causes abandonment of wells or even fields (Curtice and Dalrymple, 2004; Wang et al., 2016). During the life of an oil field which consists of three main stages, that is exploration, development and increasing the oil recovery (IOR) or enhanced oil recovery (EOR), which requires the drilling of many wells, some wells are abandoned because hydrocarbon production is unfeasible due to high water cut ("cut" meaning share or ratio of water in the well). In addition, exploration wells which are dry are also abandoned. In addition to the abandoned wells, there are suspended wells in oil fields which are mainly caused by the price of oil and profit. It must be mentioned that before the abandonment of high water cut wells, they are suspended by operator companies for 6-12 months in the attempt to find infrastructure or other profitable circumstances that enforces them to reactivate the wells. After this period, the wells must be abandoned carefully following local policies to minimize surface and subsurface contamination (Alboiu and Walker, 2019). Alboiu and Walker (2019) gathered data on the status of wells in Alberta province in Canada (Table 1) which shows that the large number of 63,411 wells (abandoned, reclaimed and orphaned) have been abandoned. There are also reports from Texas and China which show the abundance of abandoned wells being 10,730 and 76,844, respectively (Li et al., 2015; Wang et al., 2018).

TABLE 1: Oil and gas well status in Alberta province of Canada (Alboiu and Walker, 2019)

Well type	**Number of wells**	**Precent from total (%)**
Active	143,984	47.93
Inactive but not suspended	17,527	5.83
Suspended	75,479	25.13
Abandoned	42,571	14.17
Reclaimed	17,723	5.90
Orphaned	3117	1.04
Total number of wells	300,401	

Dissolved methane, ethane, propane and salinity in oil and gas production fluids are possibly hazardous if they are emitted into the atmosphere, like methane, or leaked into groundwater resources (Bachu, 2017; Boothroyd et al., 2016; Jackson et al., 2013). By measuring the methane emission into the atmosphere, studies across the entire USA indicated that the suspended and abandoned wells emit a significant volume of methane hourly, which could also be found in groundwater (Kang et al., 2016; McMahon et al., 2018). Results showed that the mean methane emission from unplugged and plugged wells in the USA were estimated to be 1.0×10^4 and 2 mg/h, respectively (Townsend-Small et al., 2016). Recently, it was shown that completed methane protection plugging costs $37,000 per well, which could be justified considering air quality, climate change and social consideration costs (Kang et al., 2019).

As mentioned, management of large volumes of co-produced water and abandonment of suspended wells imposes environmental and economic issues for production companies. Besides co-produced water management challenges such as providing the required injection facilities for disposing (well, pump, transportation, etc.) (Ramirez, 2010; Skalak et al., 2014), environmental policies must be considered to prevent groundwater and subsurface layers from getting polluted (Lee and Neff, 2011; Estrada and Bhamidimarri, 2016; Zhang and Hascakir, 2021). Therefore, oil and gas companies have commenced to use the accessible geothermal energy in the subsurface to find solutions for economic problems such as reservoir shrinkage, production cost increase and oil price fluctuations (Burnett, 2004; Sirivedhin et al., 2004; Guerra et al., 2011; Sedlacko et al., 2019). Furthermore, harnessing the stored geothermal energy in oil fields allows them to take steps towards a more green way of energy production, to reduce operation costs, increase profits of mature fields and attain benefits for nature protection and anti-global warming achievements (Alimonti et al., 2021). Therefore, both direct and indirect (electricity generation) geothermal utilization have been studied and installed in some oil fields to extend the economic life of the fields (Nordquist and Johnson, 2012; Liu et al., 2018).

In this report, after a thorough literature review about the estimated potential of stored geothermal energy in oil fields and current developments, the principles of electricity generation by combined gas turbine and ORC systems are reviewed, methods which are used for power generation from dissolved or free gas (methane, ethane and propane) in water.

2. GEOTHERMAL RESOURCE

2.1 Potentials of geothermal energy in oil and gas fields

The potential of stored geothermal energy in the subsurface increases with increasing depth, due to the local thermal gradient. According to this theory, conventional hydrocarbon reservoirs which are located at depths of more than 1 km could contain a great amount of geothermal energy. It has been demonstrated that the temperature is in the range of 60-150°C in conventional petroleum reservoirs, while natural gas reservoirs usually have higher temperatures than oil reservoirs (Liu et al., 2018). The abundant geothermal resources in oil and gas reservoirs have been investigated by studies around the world. In the UK, a GIS temperature study has investigated the repurposing of existing oil wells for geothermal energy production (Figure 2). It showed that there are 2,242 onshore hydrocarbon wells of which 560 wells are suitable to be repurposed and 292 are currently in operation. Similarly, by using aggregated water production data for all operating wells in each field, the Wytch Farm and Wareham fields have been identified to have the greatest potential for geothermal repurposing. Wytch Farm is the largest onshore oil field in western Europe which produces co-produced water at ~65°C that might result in a feasible thermal power output of ~90 MW_{th} (Watson et al., 2020).

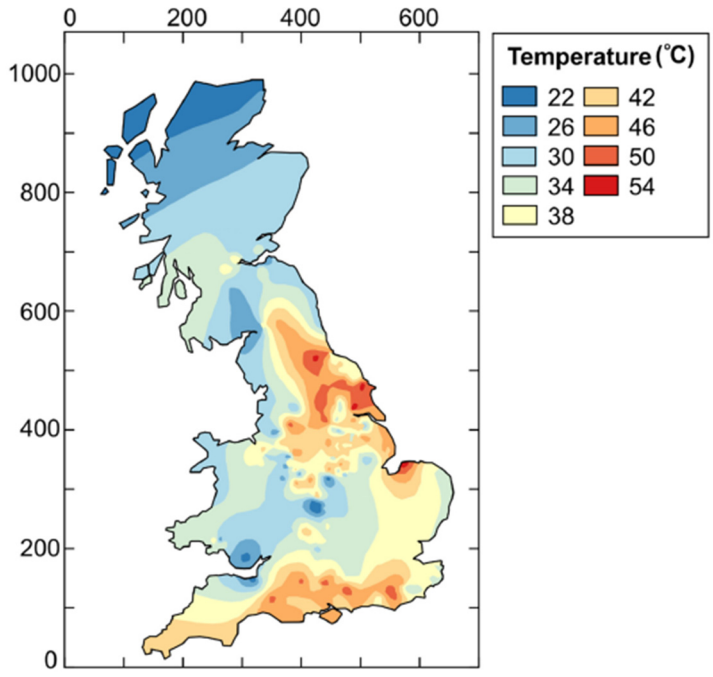

FIGURE 2: Regional temperature variation at 1 km depth across the UK (Watson et al., 2020)

Augustine and Falkenstern (2014) mapped the temperature distribution of the lower 48 US states at a depth of 3500 m and demonstrated intermediate to high temperatures in areas with oil and gas activities, such as Texas, Oklahoma, Louisiana, and North Dakota. As the study of Tester et al. (2006) confirms, some wells in Texas, Oklahoma and Louisiana have relatively high temperatures (150°C-200°C) at the bottomhole depth. In the state of Texas alone, there are tens of thousands of wells with bottom hole temperatures of over 121°C, some reach up to 204°C (Erdlac et al., 2007). Other surveys have been carried out around the world, e.g., in Turkish and Italian mature oilfields (Kaplanoğlu et al., 2020; Alimonti et al., 2021). Major hydrocarbon basins in China were also reported to be rich in geothermal resources, such as Daqing oil field, Liaohe oil field, and Huabei oil field, where the total reserves were estimated to be up to 424 EJ (1EJ = 10^{18} J) of recoverable geothermal energy as shown in Table 2 (Wang et al., 2016).

TABLE 2: Value of stored and recoverable geothermal energy in the greatest Chinese oilfields (Wang et al., 2016)

Oilfield	Total geothermal energy (EJ)	Recoverable geothermal energy (EJ)
Hubaei	7100	306
Daqing	2900	89
Liaohe	1010	29
Total	11,010	424

The water-to-oil (WOR) and water-to-gas (WGR) ratios are indicators used to quantify the volume of co-produced water compared to the volume of produced oil or gas. Globally, the average WOR was about 3:1 in the 2000s (Khatib and Verbeek, 2003) and is recently closer to 4:1, but based on the factors such as field history, the type of hydrocarbon and the technologies employed, it can range between 0.4 to 36 locally (Veil, 2015). At the world scale, the WOR index has been increasing because conventional hydrocarbon reservoirs are maturing. Therefore, they produce less hydrocarbons but higher volume of water (Veil et al., 2004; Healy et al., 2015). The estimated volume of co-produced water across the world has increased by more than 78% between 1990 and 2015 from about 10.6 billion m^3 to 18.9 billion m^3 compared to a 38% growth of oil production from 3.7 billion m^3 to 5.1 billion m^3. This trend is expected to continue and predictions say that the volume of globally produce water will be between 29 and 54 billion m^3 in 2020 (Echchelh et al., 2018). Although little information is available from oil and gas producing industries, reports say that notable volumes of co-produced water from hydrocarbon reservoirs are produced in arid regions that suffer from water shortages (Guerra et al., 2011; Echchelh et al., 2018). The rock and fluid characteristics of reservoirs could affect the volume of co-produced water and changes over time. For instance, higher porosity, permeability and lower compressibility of oil are the reasons why oil reservoirs commonly produce larger volumes of water than gas reservoirs (Guerra et al., 2011).

2.2 Advantages of extracting the stored geothermal energy in hydrocarbon fields

Wang et al. (2018) summarized the advantages of harnessing geothermal energy in hydrocarbon fields as being cost effectiveness, risk reduction, abundant market in oil and gas fields and government support that are described below.

As mentioned before, because there are numerous tested wells with great integrity, there is no or little requirement to drill new wells or retrofit the old wells. Therefore, the cost of conventional geothermal projects could be reduced by as much as 50 percent. Also, because oil and gas fields have access to service roads, wellsite facilities and pipelines, the initial investment could be reduced.

As mentioned in the introduction, risks of geothermal projects are highest at the exploration and drilling stage. Not only is the risk of drilling eliminated, but there are also long-term exploration and production data which were used to investigate the reservoir characteristics and predict its behaviour during field development. Therefore, by interpretation of the existing data, uncertainties could be reduced making decision making easier.

Extracted geothermal energy might find an abundant market at the oil and gas fields which currently need large volumes of the produced fossil fuels to provide heat and electricity for space heating, oil gathering systems and EOR processes. For example, only two oil gathering systems in the north of China which dehydrate oil and reduce the viscosity of crude oil spend around $503,000 per year for providing the required energy.

2.3 Utilization methods and current development

History of utilization of geothermal energy around the world dates back to when native Americans, Icelanders, Japanese and others used thermal energy of hot springs for cooking, bathing and heating. Through technological advancement in the 20th century, both direct utilization of geothermal energy and power generation have been introduced (Lund, 2000). Typically, the produced heat from geothermal resources provides the required energy to generate electricity or can be used directly as a heat source for different purposes which depend on the temperature of geothermal resources (Soltani et al., 2019). Geothermal energy is also used for electrical power production. Single and double flash cycles are well-known technologies for electricity generation from high enthalpy reservoirs which have temperatures of over 150°C (DiPippo, 2015; Moya et al., 2018). For geothermal resources in oil fields, which are of low to intermediate temperature, there are case studies and research which suggest that binary power plants such as Organic Rankin Cycles (ORC) are an appropriate option (Li et al., 2012; Soltani et al., 2019; Yang et al., 2017).

Non-electricity purposes of geothermal utilization take advantage of the produced heat for applications requiring temperatures of less than 150°C. Geothermal utilization of oil fields has a long history in European countries such as Austria, where heat produced from abandoned oil exploration wells has been utilized for spa resorts. Similarly, in Albania, the heat required for greenhouses is supplied by abandoned wells which have temperatures of over 65°C. In Hungary, water flooding as a secondary oil production method and the heating of gathering pipes in heavy oil production have been implemented as ways to use the geothermal water (Lund and Boyd, 2016). Since 2002, China has utilized the geothermal potential at Shengli oil field for house heating and oil gathering heat tracing systems. The total saved energy in the residential area is up to 10.3 EJ (EJ = 10^{18}J) which has prevented the burning of 3×10^4 tons of coal or 2×10^4 tons of oil between 2002 and 2012, resulting in the reduction of 9.8×10^8 tons of carbon dioxide and 500 tons of sulfur dioxide emissions (Liu et al., 2014; Chandhana et al., 2018). Wang et al. (2016) reviewed other Chinese oil fields which utilize stored geothermal energy. In Huabei oil field, a heat-trace oil gathering system and crude oil transportation have been installed by retrofitting two abandoned wells which provide 600 m^3/day of thermal water at 100-110°C and results in conserving approximately 5 tons of oil and 3500 m^3 of gas daily. Daqing, Liaohe and Zhongyuan oil fields also extract geothermal energy from the co-produced water for space heating and crude oil transportation purposes (Wang et al., 2016).

Organic Rankin cycle power plants generate electricity from intermediate and low temperature geothermal resources like oil fields (Li et al., 2012; Liu et al., 2015; Ahmadi et al., 2020; Zhang et al., 2021). Even though numerous simulations investigate the performance of ORC power plants at oil fields (abandoned wells and co-produced water) (Noorollahi et al., 2015; Hu et al., 2017; Yang et al., 2017; Nian and Cheng, 2018), there are only three implemented examples worldwide that utilize this technology to generate electricity from high temperature co-produced water (Wang et al., 2018). As shown in Table 3, in the USA, there are two implemented projects. One is in the Wyoming oil field where an ORC power plant generates 180 kW of electricity from co-produced water (Nordquist and Johnson, 2012). The other is the first commercial project which is located in North Dakota where net power generation equal to 250 kWe has been realized (Gosnold, 2017). Also, China uses co-produced water with a temperature of 110°C to generate net power of 310 kW_e (Xin et al., 2012).

TABLE 3: Examples of ORC power plants utilizing water produced from oil fields (Wang et al., 2018)

Oilfield	Temperature [°C]	Flowrate [Kg/s]	Net power output [KWe]	ORC Efficiency [%]
Wyoming, USA	76.6	73.6	132	4.27
North Dakota, USA	98	55.2	250	3.85
Huabei, China	110	33.33	310	5-6.8

2.4. Characteristics of geothermal resource in this study

In Figure 3 it is shown that Iran has 95 developed oil and gas fields with high numbers of drilled wells. Most of the Iranian fields have produced hydrocarbons for more than two decades and operational companies are struggling with the large volume of co-produced water. Right now, they only inject the produced water into the reservoirs to maintain the pressure without any heat recovery systems. Based on available data, some of the oil and gas fields in Iran have giant aquifers under the hydrocarbon layers. Therefore, high-pressure water with temperatures of more than 60°C is commonly produced. It must be mentioned that in some gas fields such as Khangiran gas field (Number 95 on Figure 3), the wellhead temperature of co-produced water reaches 90°C and more (Javadi et al., 2020).

FIGURE 3: Iranian oil and gas fields (Javadi et al., 2020)

Due to the high pressure and temperature of reservoirs, only small amounts of hydrocarbon gases (methane, ethane propane etc.) have been dissolved into the water and most of them are released by pressure drop inside the well and at the wellhead (Danesh, 1998).

ORC power plants require a feed stream with temperatures of near to or more than 100°C to generate electricity efficiently. Since this study looks at power generation from high water cut oil and gas wells which produce gas and geothermal water with temperature of more than 90°C, we consider a combined gas turbine and ORC system which recovers the heat of the gas exhaust to increase the temperature of the geothermal water and prepares it for the ORC.

Temperature and flow rate assumptions are based on available data from around the world (USA and China). The flow rate of co-produced water is estimated by choosing a value inside the range of observed values and the characteristics of the geothermal resource assumed are listed in Table 4. Also, there are two mass flowrate percentages used for natural gas (1% and 0.2% of total flow rate) based on gas solubility in water at reservoir conditions.

It must be mentioned that the co-produced water has a high salinity which might affect the design and application of utilization systems and causes a reduction in the heat capacity of the brine.

TABLE 4: Fluid and well parameters considered in this study

Wellhead temperature	94 [°C]
Flow rate of fluid (water + gas)	50 [kg/s]
Percentages of gas flow rate	1 and 0.5 % of total flow rate
Specific heat capacity	3.8 [kJ/kg/K]

3. PROPOSED WORKING CYCLES

3.1 Gas turbine

Gas turbines are common power generators which are implemented in power generation systems and propulsion cycles. There are two types of gas turbines, that is internal and external combustion machines, of which internal combustion systems are more commonly used in propulsion cycles. Based on their applications, the power capacity of gas turbines is in the range of 500 kW to 250 MW. Because of the high-power density of gas turbines, they are widely used for high power applications compared to reciprocating engines. The advantage of gas turbines is that there is no reciprocating and rubbing components inside the turbine, which makes them more reliable than reciprocating engines (Pathirathna, 2013).

A typical gas turbine mainly consists of compressor, combustion chamber and turbine as shown in Figure 4a). The process of power generation includes air entering, which is compressed by the compressor, then it is heated up inside the combustion chamber and finally expanded through the turbine rotating the generator. The turbine produces work, and the compressor utilizes some fraction of that work. Most gas turbine systems are set up like a Brayton or Joule cycle (Pathirathna, 2013). An ideal Brayton cycle is shown in Figure 4b).

Figure 4b) shows the temperature-entropy diagram of an ideal Brayton cycle. Firstly, air is compressed in an isentropic process (point 1 to point 2), secondly, combustion heat is added to the cycle heating up the air (point 2 to point 3), and finally, the air is expanded through the turbine in an isentropic process (point 3 to point 4). In practise however, the processes of compression and expansion are not isentropic and the entropy of air is increased after both components.

The power produced by the gas turbine is sufficient to rotate both the compressor and generator. The optimized aero-derivatives gas turbine with a power capacity of less than 100 MW has the highest converting efficiency from heat to electricity which is 46% while common industrial gas turbines have an efficiency of 38% to 42% (Breeze, 2018).

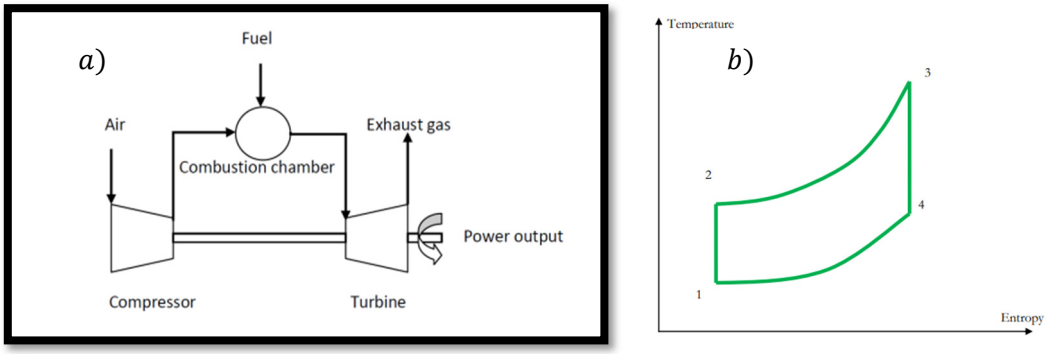

FIGURE 4: a) Typical open gas turbine (Pathirathna, 2013) b) Temperature-entropy diagram of an ideal Brayton cycle (Pathirathna, 2013)

3.2 Organic Rankine cycle (ORC)

The ORC technology is a reliable way to convert heat into electricity, which has applications in renewable energies (geothermal, biomass and solar) and industrial energy recovery. When temperature or power of the thermal source is limited and common steam and gas turbine cycles are not feasible due to economic and technical reasons, binary power plants which use special working fluid can make power generation possible. As shown in Figure 5, the power output of ORC power plants depends on the type and temperature of the resource (Macchi, 2017). Commonly, a simple single stage ORC power plant (Figure 6) consists of feed pump, vaporizer, turbine, and condenser. It has a specific working fluid with a lower boiling point than water which captures the heat from the geothermal fluid and is then expanded by the turbines to generate electricity, condensing to the liquid state before it is returned by the feed pump. All these components form a closed system so that no fluid can escape (DiPippo, 2015). Based on available data in 2017, the cumulative installed capacity of geothermal ORC power plants reached 2.7 GW_e around the world (Tartière and Astolfi, 2017). It must be mentioned that the low boiling point allows the liquid to be vaporized at a much lower temperature than water and it allows lower temperature resources to be exploited (Breeze, 2018).

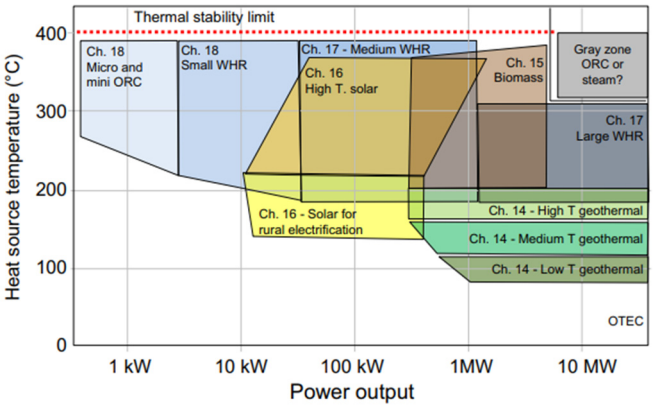

FIGURE 5: A representation of ORC application fields as a function of heat source temperature and power output (Macchi, 2017)

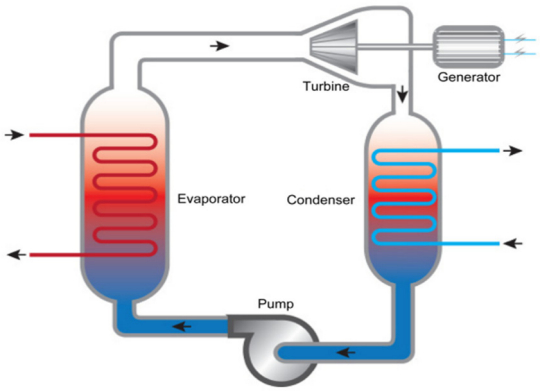

FIGURE 6: Simplified schematic of an Organic Rankin Cycle (Breeze, 2018)

Fluids commonly used in ORC-cycles are refrigerants or hydrocarbons. Liquids with high latent heat of vaporization are appropriate because they capture more heat which allows for minimization (volumetric flow) of system size. ORC turbine systems are normally available as packages ready to be linked to the heat source and the power supply. The size of such systems is relatively small. Typically, the packages are

designed for capacities between 100 kW_e and 1 to 2 MW_e although systems as large as 20 MW_e are available (Breeze, 2018).

3.3 Combined systems (gas turbine and ORC)

Most of the common heat engines that are used to generate electricity are fossil fuel based and they use heat to rotate the turbine and generators. Most of these types of power plants have efficiencies in the range of 20-40% and some modern turbines can convert heat to electricity with an efficiency of 60% (optimized aero-derivatives). That means that between 40-80% of the energy released in thermal power plants is wasted. Although a gas turbine is more efficient than a steam cycle, it releases hot gases in the atmosphere which is a result of the combustion. Temperatures of gas turbine exhaust for a high efficiency system (optimized aero- derivatives) are in the range of 400-500°C and is higher for low efficiency systems (Breeze, 2018).

Therefore, large quantities of heat are wasted through the gas turbine systems which could be used in different industrial applications. Combined heat and power (CHP) systems are thermodynamic cycles, which use the waste heat of power plants in other applications such as district heating, drying, electricity generation by means of ORC power plants etc. The simplest CHP system could be implemented by using the waste heat for drying or for a kiln (Figure 7a)). In recent decades, lots of researchers have investigated CHP systems with ORC power plants to use the waste heat of gas turbines, biomass power plants and industrial heat recovery. In these cases, the hot gases from the exhaust are combined with the ORC power plant by means of a heat exchanger. On this topic, there are lots of studies which proposed the combined CHP-ORC based systems combined with gas turbines and biomass fired plants (Figure 7b)). All of them concluded that these systems improve the efficiency, increase power output, and reduce the payback time of projects (Nami et al., 2018; Arabkoohsar and Nami, 2019; Braimakis et al., 2021).

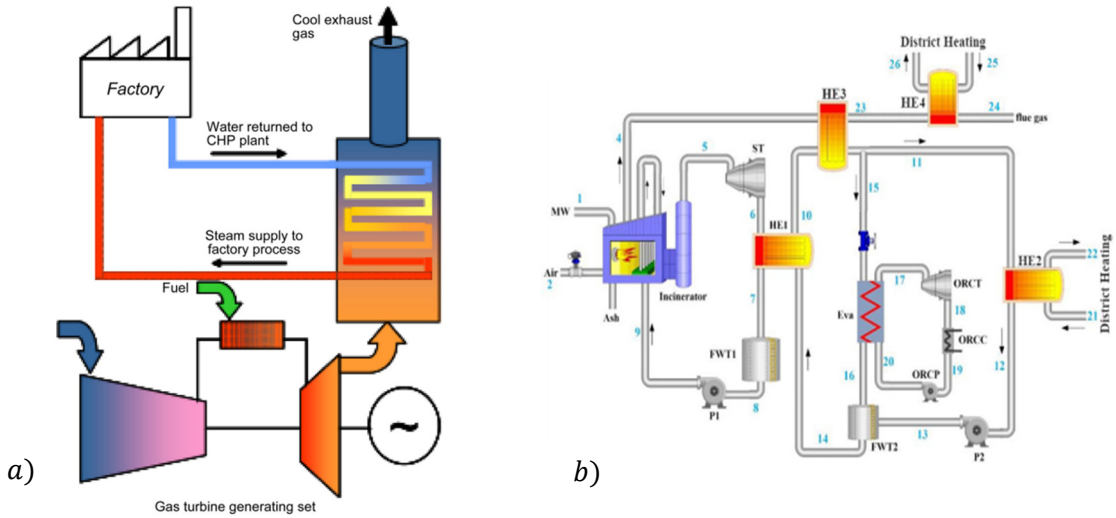

FIGURE 7: a) Schematic of using the hot exhaust gases for heating demand of factory (Breeze, 2015) b) Example of combined CHP-ORC cycle (Arabkoohsar and Nami, 2019)

Recently, Matuszewska and Olczak proposed a new combining system for low to intermediate temperature geothermal resources (temperature 80-120°C and flow rate of 100 kg/s) to use the exhaust heat of gas turbine to increase the temperature of the geofluid to enhance the efficiency of an ORC power plant (Figure 8). They concluded that the efficiency of an ORC power plant with working fluid of R1233zd could be improved from 12.21% to 19.20% depending on the temperature of geothermal brine (Matuszewska and Olczak, 2020).

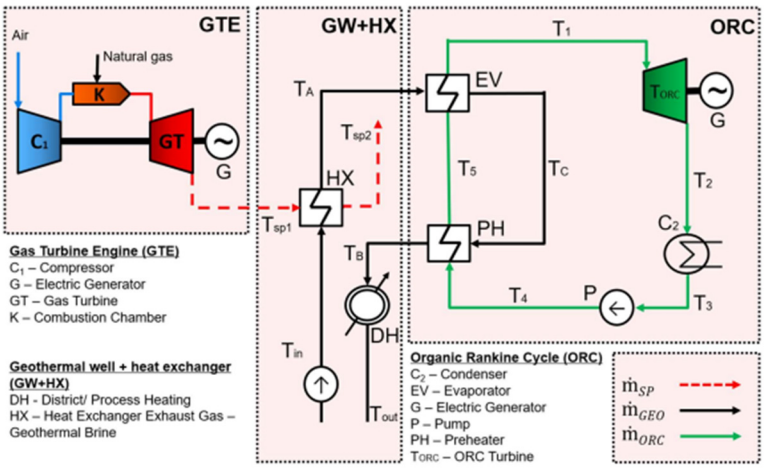

FIGURE 8: Simplified combined gas turbine and ORC power plant for low to intermediate temperature geothermal resources (Matuszewska and Olczak, 2020)

The aim of this study is proposing a combined gas turbine and ORC power plant system for high water cut oil and gas wells which produce a small volume of natural gas at the wellhead. Therefore, produced gas is burnt in the gas turbine and using the hot combustion products to heat the co-produced water which has a temperature of less than 100°C improves the efficiency of the ORC power plant. This study looks at the option of heating the geothermal fluid by hot gases from the exhaust of the gas turbine to increase the power output and to decrease CO_2 emission.

4. MATHEMATICAL AND PHYSICAL MODEL

4.1 Overview

As mentioned before, this study aims to explore the option to use both the produced gas and geothermal (co-produced) water to generate electricity. Therefore, as Figure 9 shows, a combined system which includes a gas turbine and an ORC power plant is proposed to facilitate power generation from high water cut oil and gas wells.

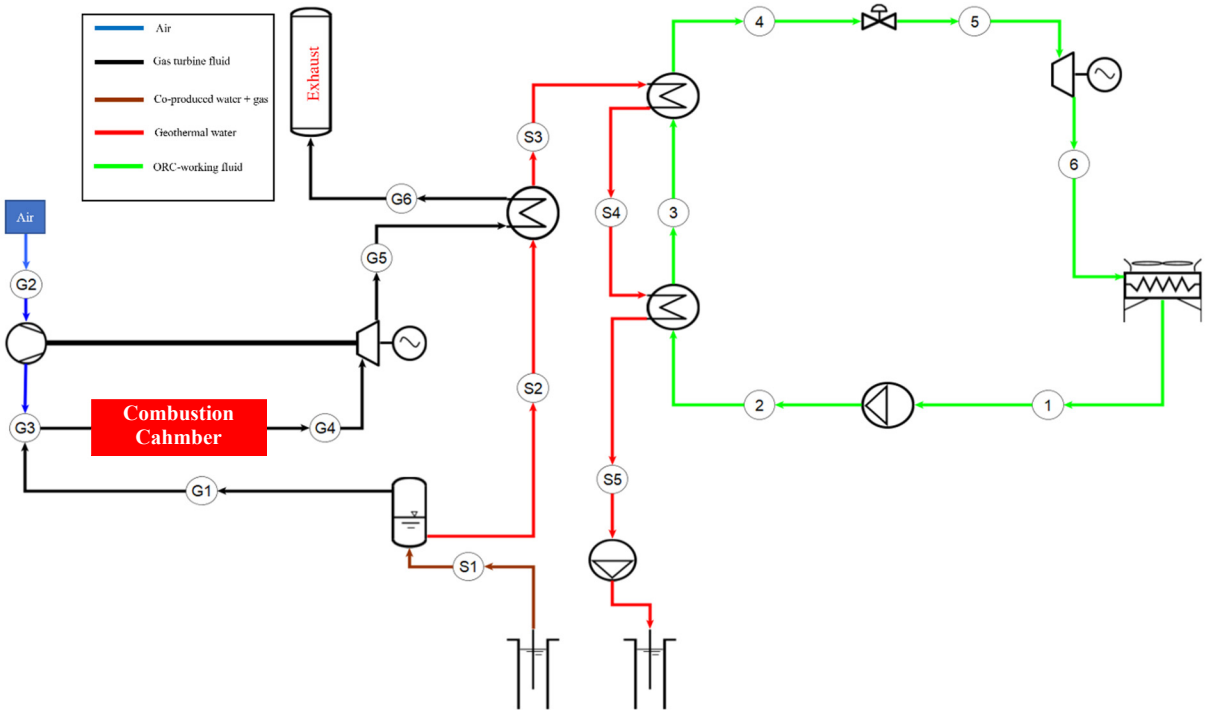

FIGURE 9: Proposed combined gas turbine and ORC

Source fluid (S1) enters the separator or degasser unit where gas (G1) and liquid (S2) are separated. On the left-hand side, the separated gas is mixed with compressed air (G2, G3) and burnt inside the combustion chamber (G4). After power generation by gas turbine, the hot exhaust gases of the turbine outlet heat up the geothermal water with a heat exchanger (G5-G6/S2-S3). On the right-hand side, working fluid starts its cycle in a liquid state after the fan (1), then it is pumped (2) to the preheater (3), vaporizer (4) and after its temperature reaches a superheated state (5), it is expanded along the turbine (6).

The thermodynamics equations of the system are solved by a program written in the Python programming language with the relevant process flow map shown in Figure 10.

In the following sections, details of the thermodynamics and calculations of the gas turbine system and ORC are covered.

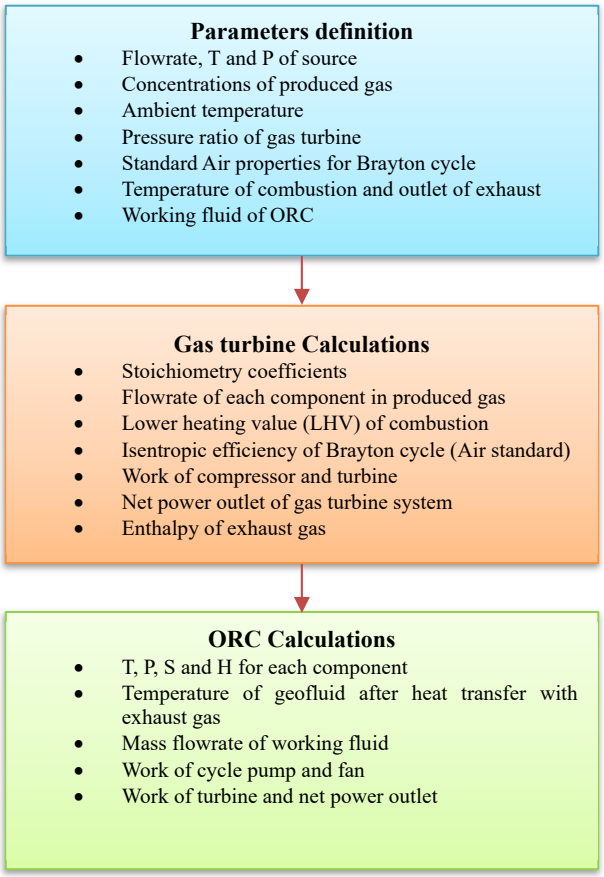

FIGURE 10: Process flow map of program

4.2 Gas turbine system

A simplified gas turbine cycle is commonly modelled by the Brayton cycle and the standard assumption is to use air as working fluid which is heated up through the combustion chamber, which uses energy produced from burning of gas at the wellhead. The general formulation for combustion of hydrocarbons is given in equation (1):

$$C_x H_y + z\,O_2 + 3.77 \times z\,N_2 \rightarrow x\,CO_2 + \frac{y}{2}\,H_2O + 3.77 \times z\,N_2 \quad (1)$$

Where x and y are the number of carbon and hydrogen atoms in the hydrocarbon component, respectively, and $z = (x + y/4)$. By using this equation and mass balance the concentrations and mass flow rates of each component are solved. Then the LHV of combustion is calculated using equation (2):

$$LHV = \sum_i \dot{m}_i \times LHV_i \quad (2)$$

Where LHV = Lower heat value of combustion [kJ/kg];
$\dot{m}_i$ = Mass flow rate of each component [kg/s];
LHV_i = Lower heat value of each component [kJ/kg].

Then power outlet of the gas turbine, W_{gt}, is calculated as shown below:

$$W_{gt} = LHV \times \eta_{is} \times \eta_{gen}/1000 \quad (3)$$

Where η_{is} is the isentropic efficiency of the gas turbine, which is calculated by temperatures of turbine outlet, T_{to}, and of the compressor outlet, T_{co}, through the equations below:

$$T_{to} = T_{ti} \times \left(\frac{1}{rp}\right)^{\frac{k}{k-1}}$$

$$T_{co} = T_{ci} \times (rp)^{\frac{k}{k-1}} \tag{4}$$

$$\eta_{is} = 1 - (\frac{T_{to} - T_{ci}}{T_{ti} - T_{co}})$$

Where W_{gt} = Outlet work of gas turbine [kW];
η_{gen} = Efficiency of generator
T_{to} = Temperature of turbine outlet [K];
T_{co} = Temperature of compressor outlet [K];
T_{ti} = Temperature of turbine inlet (temperature of combustion) [K];
T_{ci} = Temperature of compressor inlet (ambient air temperature) [K];
rp = Pressure ratio of compressor and turbine;
k = Specific heat ratio of standard air.

The net power outlet of the gas turbine can be calculated as shown below:

$$W_c = \dot{m}_{air\_c} \times (h_2 - h_1)/1000$$

$$W_{Net.gt} = W_{gt} - W_c \tag{5}$$

Where $\dot{m}_{air\_c}$ = Flow rate of required air for combustion times 1.5 [kg/s];
W_c = Work by compressor [kW];
$h_{1,2}$ = Enthalpy of compressor inlet and outlet, respectively [J/kg];
$W_{Net.gt}$ = Net power outlet of gas turbine [kW].

4.3 ORC power plant

Figure 9 shows a simplified ORC power plant diagram with its major components including condenser, cycle pump, preheater, vaporizer, main valve, and turbine. When the working fluid passes through each component, its thermodynamic properties are changed, the relevant equations for each component are given in Table 5 and the new properties are calculated using an open-source program called “coolprops”, written in the Python programming language.

After passing the condenser (point 1), the working fluid is in a liquid state and its properties can be determined using equation (6). Then, the fluid enters the pump which increases the enthalpy, pressure and entropy of the fluid (point 2 to point 3). In this process, pressure must be equal to the pressure in the vaporizer. Therefore, by calculating the specific volume, pressure difference and the new enthalpy, the temperature, enthalpy and entropy of pump outlet can be calculated by equation (7).

Then, the fluid proceeds to the preheater (point 3 to point 4) which increases the temperature of the working fluid until it reaches its boiling point temperature minus a margin temperature by transferring heat from the source water, which ends up having a lower temperature after the vaporizer. So, by calculating the properties of the working fluid at its boiling point and by assuming equal pressure in the vaporizer, equation (8) can be used to calculate the enthalpy, entropy and pressure of the working fluid at the outlet of the preheater. In the vaporizer, hot source water increases the temperature of the working fluid until it reaches a superheated state (point 4 to point 5) and equation (9) determines the fluid properties after the vaporizer.

After passing point 5 point 6, the fluid passes a main valve in the same enthalpy process, therefore, pressure is decreased and the temperature and entropy can be calculated using equation (10). Finally, the superheated working fluid is expanded by the turbine which is not isentropic (point 5 to point 6). By assuming that the outlet pressure of the turbine equals the pressure of the condenser or cooling tower, the new enthalpy and entropy are determined by equation (11).

TABLE 5: The known variables and equations for working fluid properties inside each component of the ORC

Component	Point No**.**	**Known variables**	**Calculated variables by coolprops**	**Eq. no**.
Condenser	1	$T_1 = T_{condensation}$ $X = 0$	$P_1, h_1 \; and \; s_1 \; @ \; T_1 \; and \; X$	(6)
Cycle pump	2	$P_2 = P_{vaporizer}$ $X = 0$	$v @ P_2 \; and \; X$ $dh = v \times (P_2 - P_1)$ $h_2 = h_1 + dh$ $T_2 \; and \; s_2 \; @ \; h_2 \; and \; P_2$	(7)
Preheater	3	$P_3 = P_{vaporizer} \; and \; X = 0$ $T_3 = T_{bubble} - T_{margin}$	$T, \; h \; and \; s \; @ \; bubble \; point$ $h_3 \; and \; s_3$	(8)
Vaporizer	4	$P_{dew} = P_{vaporizer} \; and \; X = 1$ $P_4 = P_{vaporizer}$ $T_4 = T_{dew} + T_{superheat}$	$T, \; h \; and \; s \; @ \; dew \; point$ $h_4 \; and \; s_4$	(9)
Cycle valve	5	$h_5 = h_{in}, \;\; P = P_{vaiporizer} - dp_{45}$	$T_5 \; and \; s_5$	(10)
Turbine	6	$P_6 = P_{cond_{out}}$	$h_s @ P_6 \; and \; s_{Turb_{in}}$ $h_6 = h_5 - (\eta_{turb}(h_5 - h_s))$ $s_6 \; and \; T_6$	(11)

Where T = Temperature of working fluid at each point [K];
X = Quality or concentration of vapour phase in two phase fluid;
P, dp = Pressure/pressure drop of working fluid at each point [Pa];
h = Enthalpy of working fluid at each point [J/kg];
s = Entropy of working fluid at each point [J/kgK];
v = specific volume of fluid [m^3/kg];
T_{dew} = Temperature of working fluid at dew point [K];
T_{bubble} = Temperature of working fluid at boiling (bubble) point [K];
$T_{superheat}$ = Assumed temperature increase after bubble point at the vaporizer [K];
η_{turb} = Efficiency of ORC turbine;
h_s = Isentropic enthalpy of turbine [J/kg].

After calculating the thermodynamic properties of the ORC working fluid, the enthalpy of source water at each point and the increased temperature after contact with the exhaust gas must be determined (Table 6). Based on the diagram in Figure 9, the source water has a specific temperature and pressure at the wellhead (point S1 and equation (12)). Then, it passes through a degasser or a separator the gas is separated from the brine at a specific pressure which depends on the solubility of the gas (point S1 to point S2). In this case, based on the solubility of the gas at reservoir condition and inside the saline brine, it is assumed that the gas is released during the production through the well (Danesh, 1998).

Therefore, a simple degasser with high operational pressure or a low-pressure separator (13 bar) can be used to separate the gas (Sivalls, 1987) and the new properties of the water can be determined by equation (13). After gas separation, geofluid is heated inside a heat exchanger by the hot exhaust gas from the gas turbine (point S2 to point S3) and equation (14) can be used to calculate the temperature increment. After the heat exchanger, the hot geothermal fluid reaches the vaporizer and preheater where it changes the phase of the working fluid to superheated and warms up the working fluid. Equations (15) and (16) are used to calculate the thermodynamic properties of the geothermal fluid

TABLE 6: Equations to calculate thermodynamic properties of the source water

Component	Point No.	**Known variables**	**Calculated variables by coolprops**	**Eq. no**.
Wellhead	S1	$T_{s1} = T_{Source}$, $P_{s1} = P_{wellhead}$	$h_1 @ T_{s1}$ *and* P_{s1}	(12)
Degasser/ separator	S2	$T_{s2} = T_{Source}$, $P_{s2} = P_{separator}$	$h_{s2} @ T_{s2}$ *and* P_{s2}	(13)
Heat exchanger	S3	$P_{s3}, T_{S2}, \dot{m}_{flue}, \dot{m}_{source}$, h_{exh1}, h_{exh2} *and* C_P $\dot{m}_{water} = \dot{m}_{source} - \dot{m}_{gas}$	$T_{s3} = T_{s2} + \frac{\dot{m}_{flue}}{\dot{m}_{water}} \frac{(h_{exh1} - h_{exh2})}{C_P \times 1000}$ $h_{s3} @ T_{s3}$ *and* P_{s3}	(14)
Vaporizer	S4	$P_{s4} = P_{sep}$ $T_{s4} = T_{wf-vap-in} + T_{pinch}$	$h_{s4} @ T_{s4}$ *and* P_{s4} $\dot{m}_{wf} = \dot{m}_{source} \times \frac{h_{s3} - h_{s4}}{1000}$	(15)
Preheater	S5	$P_{s5} = P_{sep}$ $Q_{preheater} = \dot{m}_{wf} \times \frac{h_3 - h_2}{1000}$	$T_{s5} = T_{s4} - \frac{Q_{preheater}}{C_P \times 1000}$ $h_{s5} @ T_{s5}$ *and* P_{s5}	(16)

Where $\dot{m}_{flue}$ = Mass flow rate of exhaust gas from gas turbine [kg/s];
$\dot{m}_{Water}$ = Mass flow rate of geothermal water after gas separator [kg/s];
$\dot{m}_{source}$ = Mass flow rate of geothermal water at the wellhead [kg/s];
$\dot{m}_{gas}$ = Mass flow rate of produced gas from separator [kg/s];
$\dot{m}_{wf}$ = Mass flow rate of working fluid in ORC [kg/s];
$h_{exh1,2}$ = Enthalpy of exhaust gas at inlet and outlet of heat exchanger [J/kg];
C_P = Specific heat of geothermal water (due to high salinity, it is 3.8) [kJ/kg/K];
T_{Pinch} = Pinch temperature of vaporizer [K];
$T_{wf\_vap\_in}$ = Temperature of working fluid at inlet of vaporizer [K].

After calculating the thermodynamic properties of the fluid at each point, work and heat of the components are determined based on Table 7.

TABLE 7: Equations for calculating work and heat for each component of the ORC

Component	**Equation**	Eq No.
	Work [kWe]	
Cycle pump	$W_{Cycle-pump} = \frac{\dot{m}_{wf}}{\rho_{wf@(T_1,P_2)}} \times \frac{P_2 - P_1}{\eta_{pump} \times 1000}$	(17)
Injection pump	$W_{inj\_pump} = \frac{\dot{m}_{water}}{\rho_{w@(T_{s5},P_5)}} \times \frac{P_{inj} - P_5}{\eta_{pump} \times 1000}$	(18)
Fan Work	$\dot{m}_{air} = \dot{m}_{wf} \times \frac{h_6 - h_1}{h_{air2} - h_{air1}}$ $W_{fan} = \frac{\dot{m}_{air}}{\rho_{air@(T_2,P_{atm})}} \times \frac{dp_{fan}}{\eta_{fan} \times 1000}$	(19)
Turbine	$W_{turb} = \dot{m}_{wf} \times \frac{h_5 - h_6}{1000} \times \eta_{turb}$	(20)
	Heat [kW$_{th}$]	
Heat exchanger	$Q_{hex} = \dot{m}_{flue} \times \frac{h_{exh1} - h_{exh2}}{1000}$	(21)
Vaporizer	$Q_{vap} = \dot{m}_{water} \times \frac{h_{s3} - h_{s4}}{1000}$	(22)
Preheater	$Q_{pre} = \dot{m}_{wf} \times \frac{h_3 - h_2}{1000}$	(23)
	Efficiency [%]	
ORC	$\eta_{ORC} = W_{netORC}/(Q_{vap} + Q_{pre})$	(24)
Overall system	$\eta_{power\ plant} = W_{net-power\ plant}/(Q_{vap} + Q_{pre})$ $\eta_{co-generation} = (W_{net-power\ plant}/(Q_{vap} + Q_{pre})$	(25)

Where $W_{Cycle-pump}$ = Required work for cycle pump [kW_e];
W_{inj_pump} = Required work for injection pump [kW_e];
ρ_{wf} = Density of working fluid [kg/m^3];
η_{pump} = Efficiency of pumps;
ρ_w = Density of working fluid [kg/m^3];
P_{inj} = Injection pressure [Pa];
$\dot{m}_{air}$ = Air mass flow rate for fan [kg/s];
$h_{air1,2}$ = Enthalpy of air at the inlet and outlet of dan [K];
W_{fan} = Required work for fan [kW_e];
ρ_{air} = Density of air [kg/m^3];
W_{turb} = Work of turbine to surrounding [kW_e];
Q_{hex} = Heat rate through the heat exchanger [kW_{th}];
Q_{vap} = Heat rate through the vaporizer [kW_{th}];
Q_{pre} = Heat rate through the preheater [kW_{th}];
η_{ORC} = Efficiency of ORC;
$\eta_{Power\ plant}$ = Overall efficiency of combined power plant [%].

Finally, the amount of CO_2 produced per kWh can be determined as follows:

$$CO_2 = \frac{\dot{m}_{CO_2} \times 3600}{W_{net}} \tag{26}$$

Where CO_2 = Mass flow rate of produced CO_2 from power plant [kg/kWh];
$\dot{m}_{CO_2}$ = Mass flow rate of produced CO_2 from gas power plant [kg/s];
W_{net} = Net power outlet of power plant [kW_e].

There are two pumps for circulating the working fluid and injection of the geothermal fluid into the reservoir, which consume electricity and are described by equations (17) and (18), respectively. The fan also needs electricity to cool down the working fluid and is described by equation (19). The turbine of the ORC section produces work described by equation (20). Equations (21) to (23) determine the heat transferred inside the heat exchanger, vaporizer, and preheater, respectively.

5. RESULTS AND DISCUSSION

5.1 Overview

In this section, three different cases are modelled, a single gas turbine cycle and two combined gas turbine and ORC systems with different mass flow rates of gas. The results are compared with each other. Then, a sensitivity analysis is studied to investigate the effect of source temperature on the output and characteristics of the system. At last, to increase the overall efficiency of the system, the effect of adding a direct heat utilization unit into the system is analysed.

5.2 Gas turbine

As mentioned in previous sections, a single gas turbine cycle uses the separated gas from the well and compressed air to generate electricity from the produced heat from gas combustion at the combustion chamber. A detailed diagram of the gas turbine cycle can be found in the appendix (Appendix Figure A1). In this case, the flow rate of natural gas is assumed to be 0.5 kg/s (1% of wellhead stream). Results show that a gas turbine with a pressure ratio of 11 can generate 8,360 kW_e from gas combustion where the compressor uses 4,980 kW_e of the generated power to compress the air.

Therefore, a gas turbine with isentropic thermal efficiency of 49.6% generates 3,560 kW_e net power with an overall efficiency of 14.5% from 24,600 kW_{th} energy of gas combustion which emits about 1.42 kg CO_2 per kWh.

5.3 Combined cycles of gas turbine and ORC

Two combined systems, which use exhaust of the gas turbine to heat up the geothermal fluid, are also considered. In these cases, the mass flow rate of the produced gas is assumed to be 0.5 kg/s (1% of wellhead stream) and 0.25 kg/s (0.5% of wellhead stream). Thermodynamic diagrams and details of calculations are shown in Figures A2 and A3 in the Appendix.

Results for the net power outlet of the ORC and net power outlet of the combined power plant (Figure 11) show that the ORC can generate 626 and 385 kW_e net electricity from geothermal fluid, which is heated through heat transfer from exhaust gas from combustion with 0.5 and 0.25 kg/s of gas, respectively. Also, it is obvious that by decreasing the amount of input gas, the power outlet of both the gas turbine and ORC is reduced.

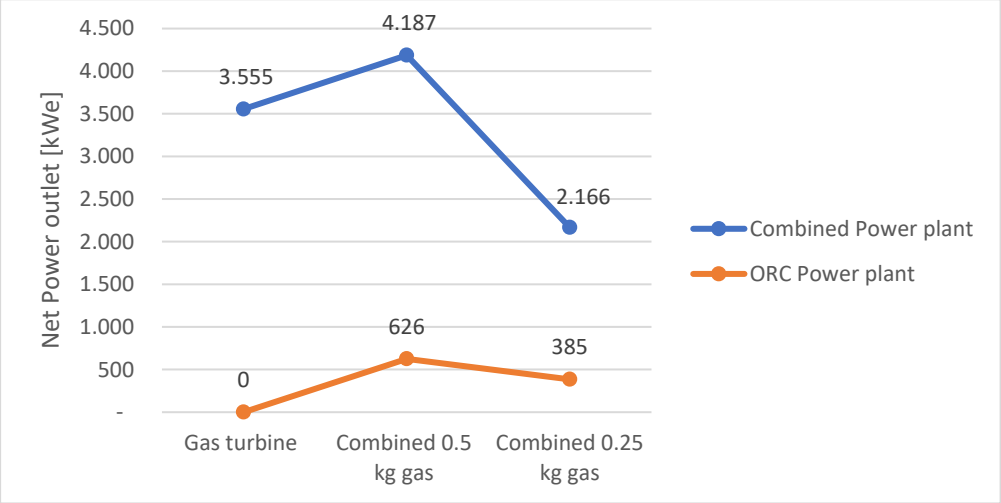

FIGURE 11: Power outlet of ORC and combined power plant for different scenarios

Figure 12 shows that combining an ORC with a gas turbine decreases the overall efficiency of system. Comparing the values of case 1 and case 2 which use the same flow rate of gas in the gas turbine shows a decrease from 14.5% to 9.5% which is similar to that of a low efficiency ORC. This figure also shows that a reduction of gas mass flow rate leads to a lower temperature geofluid and consequently lower ORC efficiency.

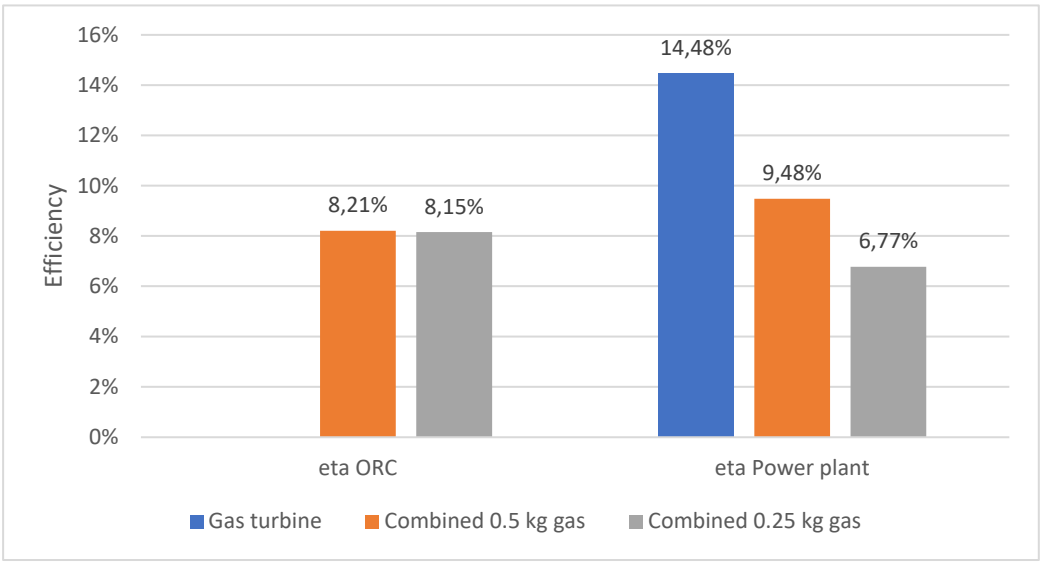

FIGURE 12: Efficiency of ORC and combined power plant

As Figure 13 shows, case 1 (single gas turbine) produces 1.42 kg CO_2 per kWh which basically depends on the gas flow rate. The combined cycle of case 2 reduces the CO_2 production to 1.20 kg per kWh (14.9%) by using green geothermal energy. But case 3, with a smaller flow rate, reduces the amount of CO_2 per kWh to 1.17, corresponding to a reduction of 17.8%.

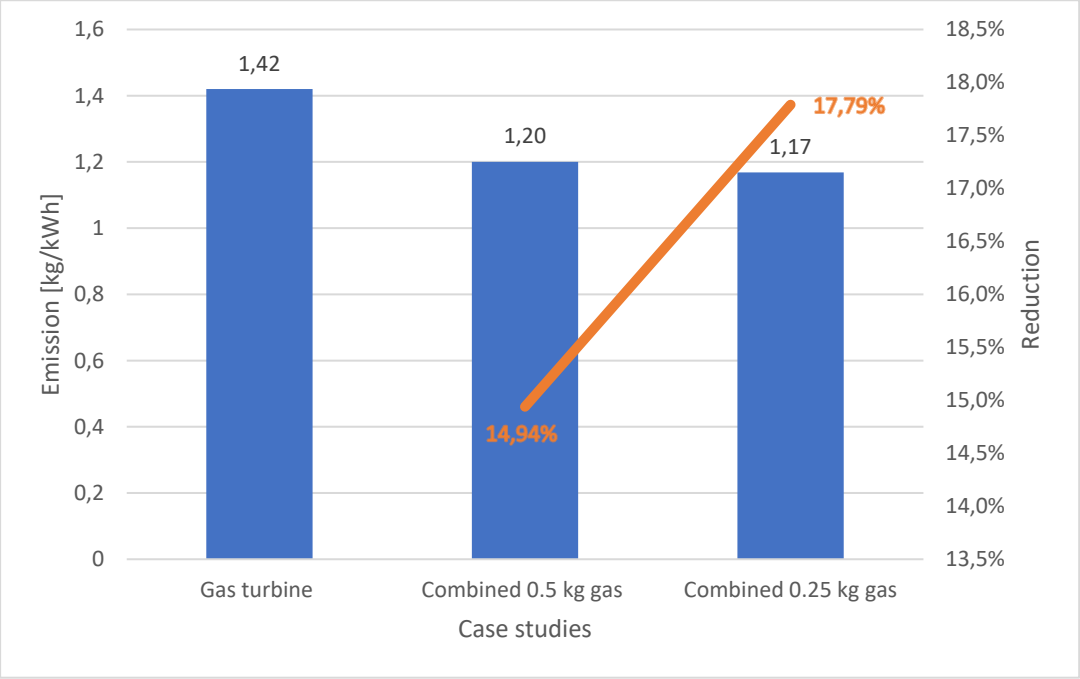

FIGURE 13: CO_2 emission per kWh for different scenarios

5.4 Sensitivity analysis

The temperature of the co-produced water plays an important role in power generation from geothermal resources in oil and gas fields. Commonly, the temperature of co-produced water is in the range of 70-120°C at the wellhead. Therefore, in this section, two higher and lower temperature sources are modelled using the case 2 scenario. It is obvious that by increasing the source temperature, geothermal equity in power generation increases and Figure 14 shows that this can vary from 3.84% to 26.6% for temperatures of 75°C and 120°C, respectively.

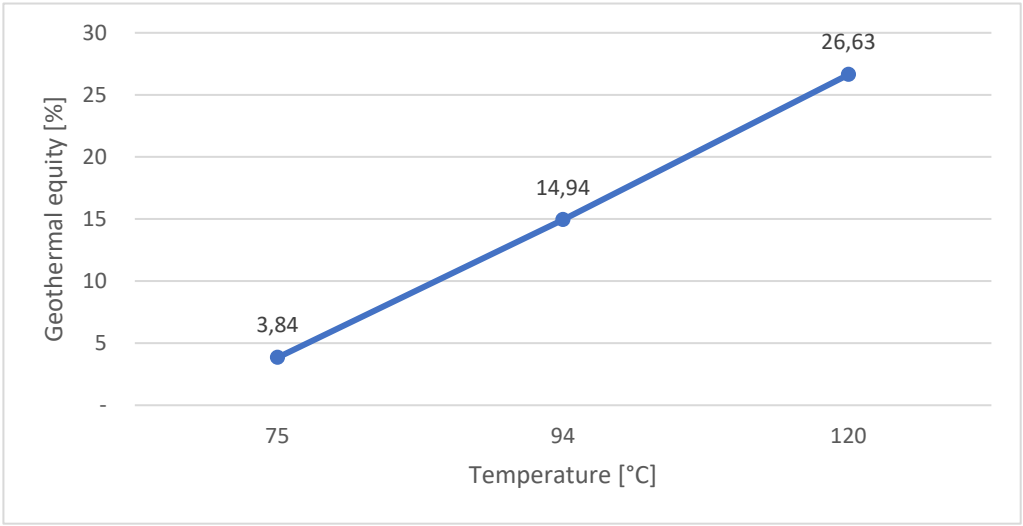

FIGURE 14: The geothermal equity in power generation for different source temperatures

The results show that the exhaust gas can increase the temperature of geothermal fluid by 18.9°C. Therefore, as Figure 15 shows, the power outlet of the ORC decreases from 1290 kW_e to 142 kW_e when the source temperature is reduced from 120°C to 75°C, which affects the net power generation of the combined system. Figure 16 shows that the efficiency of the ORC power plant is dependent on the source temperature and is 8,25% for geothermal fluid with a temperature of 120°C and is reduced to 7.92% when the temperature is 75°C. The overall efficiency of the power plant is reduced for the same reason.

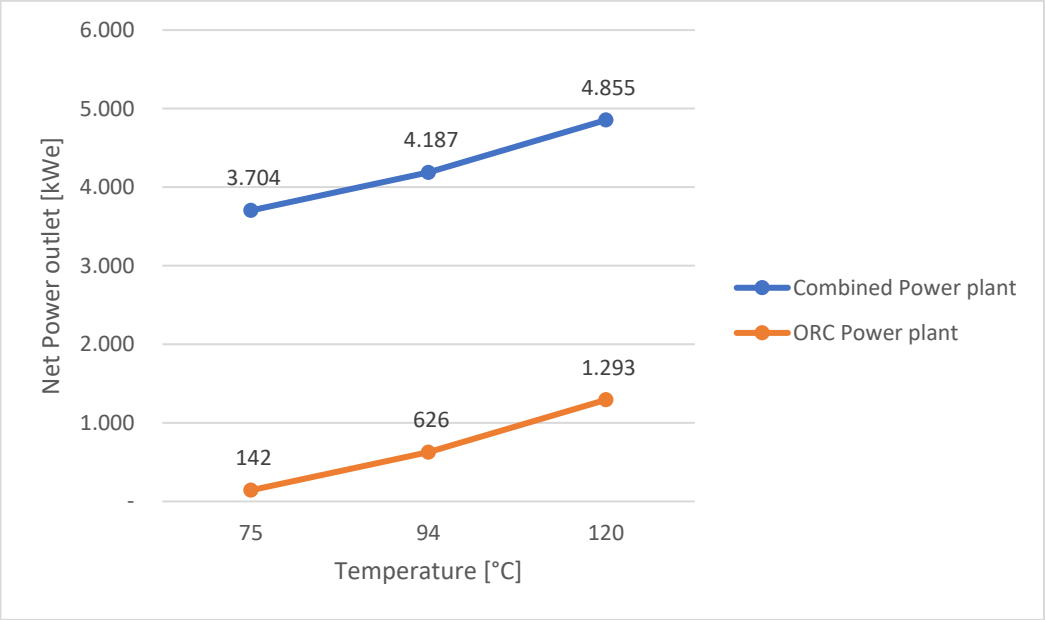

FIGURE 15: Power outlet of ORC and combined power plant for different source temperatures

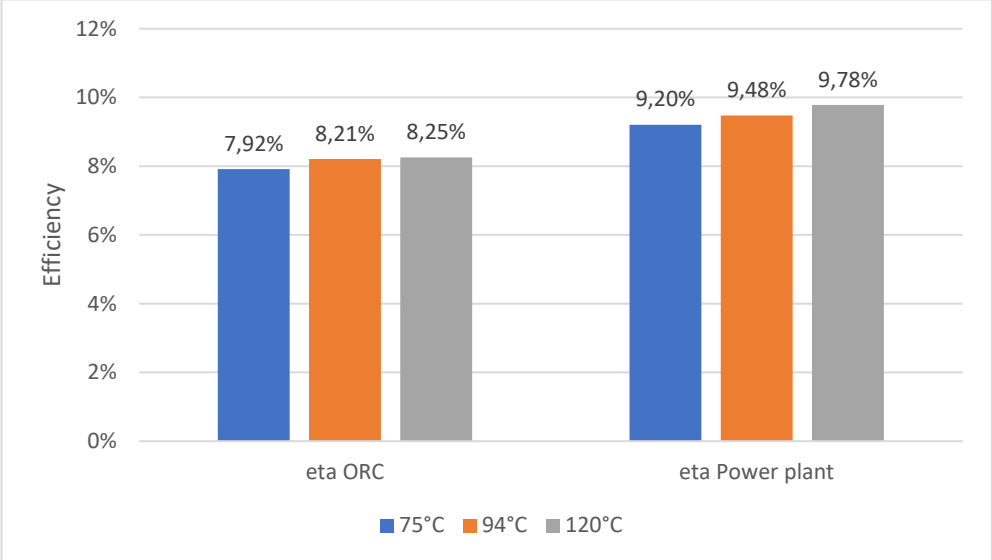

FIGURE 16: Efficiency of ORC power plant and combined system for different temperatures

Finally, Figure 17 shows that higher geothermal fluid temperature leads to higher power generation and reduction of CO_2 production per kWh of the combined system for case 1. It is shown that a temperature of 120°C maximises the CO_2 reduction per kWh (26.6%) while the lowest value (3.78%) is related to a source temperature of 75°C.

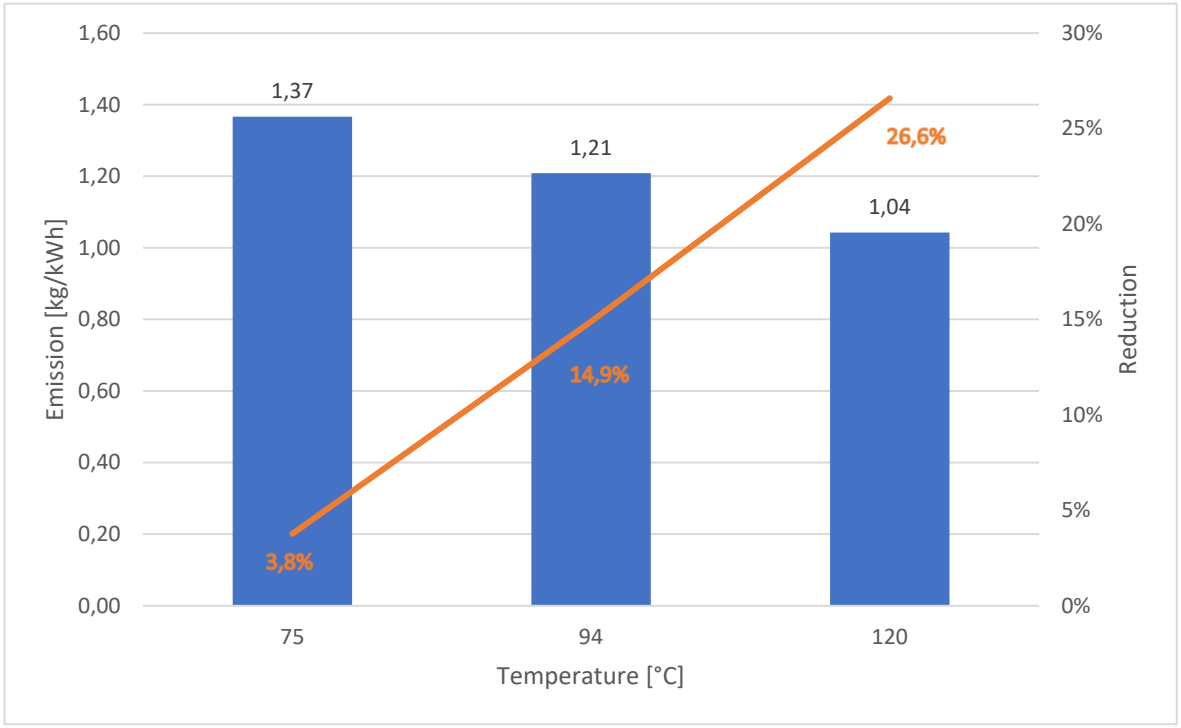

FIGURE 17: CO_2 emission of combined power plant for different source temperatures and the amount of reduction compared to case 1 (gas turbine only)

5.5 Co-generation of heat and electricity

Due to low total efficiency of the combined power plant, this part assumes a direct heating system for the source water before injection because it has a high temperature. Figure 18 shows that when a higher mass flow rate of gas is used, the temperature of the source water is increased more which leads to a higher mass flow rate of the working fluid and consequently lower injection temperature. Therefore, with regard to equation (25), the total efficiency of the co-generation system is increased for case 3 which uses less gas and therefore, has a higher injection temperature.

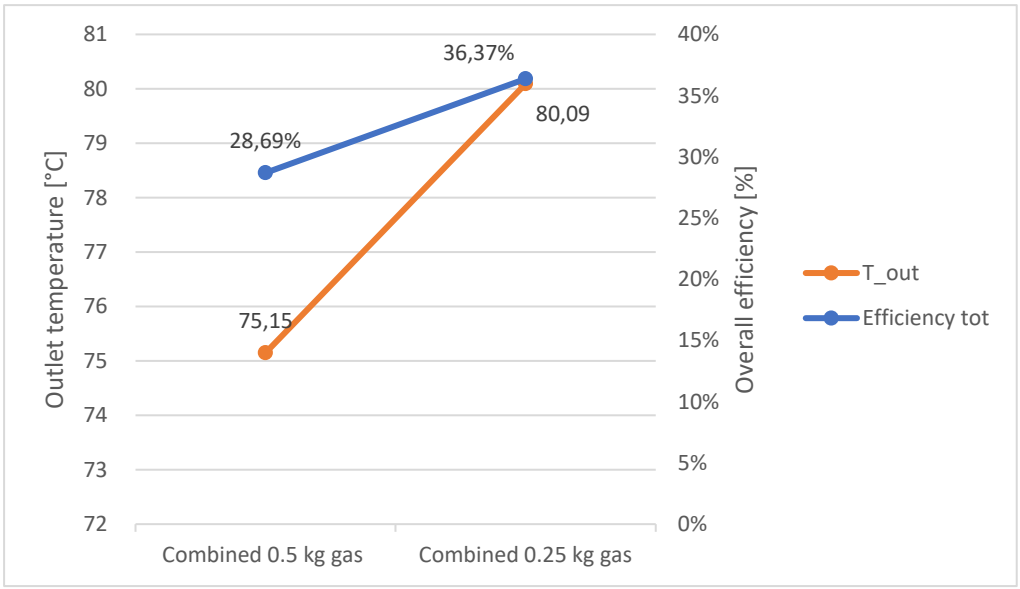

FIGURE 18: Overall efficiency of system with cogeneration of heat and electricity

6. CONCLUSIONS

In this study, after proposing a combined gas turbine and ORC system for power production from high water cut oil and gas wells, three different scenarios of electricity generation are compared. Case 1 only consists of a gas turbine but cases 2 and 3 consist of combined systems, which use the exhaust gases for heating up the geothermal water, with different mass flow rates of produced gas, to increase the power production from the ORC power plant.

The results show that the gas turbine can generate around 5 MW_e net power by using 0.5 kg/s produced gas from the high water cut well. But in cases 2 and 3, which use 0.5 kg/s and 0.25 kg/s gas, respectively, exhaust gas can heat up the geothermal water which results in higher power outlet, ORC efficiency and overall efficiency of the power plant and these changes have a direct relation with mass flow rate of the gas. In case 2 for instance, by using more gas for the combined system, power outlet and efficiency is increased. In case 3 the exhaust gas cannot warm up the geothermal water as much which is the result of a lower mass flow rate of exhaust gas. Case 3 still results in the highest reduction of CO_2 emission per kWh compared to case 1.

Another result shows that efficiencies of the ORC and power plant are dependent on the mass flow rate of gas and exhaust gas. When decreasing the flow rate of gas, mass flow rate of exhaust gas and efficiency are reduced.

Because the temperature of co-produced water varies from field to field or well to well, a sensitivity analysis was carried out to study the effect of the source temperature on net power, ORC efficiency and overall efficiencies. It demonstrates that a higher temperature resource can reduce the emission more than other scenarios and it has a higher efficiency.

Finally, with regard to the low overall efficiency of the power plant, a district heating system is installed which uses the return water before injection. It can increase the overall efficiency of the power plant that is calculated by dividing the sum of net power and directly used heat, on one hand, by total input heat from the geothermal fluid and natural gas, on the other hand.

ACKNOWLEDGEMENTS

At first, I must say thanks to all the staff of GRÓ GTP who supported us and provided great conditions for research. Then, I say thanks to dear Oskar and dear Pall for the guidance that they gave me during this project. Also, I send my best regards to dear Davar and dear Javad from Niroo Research Institute (NRI) who are my great managers. At last, I cannot forget all of the favours and support of my parents (Davoud and Shabnam), God keep them for me forever.

NOMENCLATURE

LHV = Lower heat value of combustion [kJ/kg];
$\dot{m}_i$ = Mass flow rate of each component [kg/s];
LHV_i = Lower heat value of each component [kJ/kg];
W_{gt} = Work outlet of gas turbine [kW];
η_{gen} = Efficiency of generator;
T_{to} = Temperature of turbine outlet [K];
T_{co} = Temperature of compressor outlet [K];
T_{ti} = Temperature of turbine inlet (temperature of combustion) [K];
T_{ci} = Temperature of compressor inlet (ambient air temperature) [K];
rp = Pressure ratio of compressor and turbine;
k = Specific heat ratio of standard air;
$\dot{m}_{air_c}$ = Flow rate of required air for combustion times 1.5 [kg/s];
W_c = Work of compressor [kW];
$h_{1,2}$ = Enthalpy of inlet and outlet of compressor [J/kg];
$W_{Net.gt}$ = Net power outlet of gas turbine [kW];
T = Temperature of working fluid at each point [K];
X = Quality or concentration of vapour phase in two phase fluid;
P, dp = Pressure/pressure drop of working fluid at each point [Pa];
h = Enthalpy of working fluid at each point [J/kg];
s = Entropy of working fluid at each point [J/kgK];
v = Specific volume of fluid [m^3/kg];
T_{dew} = Temperature of working fluid at dew point [K];
T_{bubble} = Temperature of working fluid at boiling point [K];
$T_{superheat}$ = Assumed temperature to increase after boiling point at the vaporizer [K];
η_{turb} = Efficiency of ORC turbine;
h_s = Isentropic enthalpy of turbine [J/kg];
$\dot{m}_{flue}$ = Mass flow rate of exhaust gas from gas turbine [kg/s];
$\dot{m}_{Water}$ = Mass flow rate of geothermal water after gas separator [kg/s];
$\dot{m}_{source}$ = Mass flow rate of geothermal water at the wellhead [kg/s];
$\dot{m}_{gas}$ = Mass flow rate of produced gas from separator [kg/s];
$\dot{m}_{wf}$ = Mass flow rate of working fluid in ORC [kg/s];
$h_{exh1,2}$ = Enthalpy of exhaust gas at inlet and outlet of heat exchanger [J/kg];
C_P = Specific heat of geothermal water (due to high salinity, it is 3.8) [kJ/kg/K];
T_{Pinch} = Pinch temperature of vaporizer [K];
$T_{wf\_vap\_in}$ = Temperature of working fluid at inlet of vaporizer [K];
$W_{Cycle-pump}$ = Required work for cycle pump [kWe];
W_{inj_pump} = Required work for injection pump [kWe];
ρ_{wf} = Density of working fluid [kg/m^3];
η_{pump} = Efficiency of pumps [%];
ρ_w = Density of working fluid [kg/m^3];
P_{inj} = Injection pressure [Pa];
$\dot{m}_{air}$ = Air mass flow rate for fan [kg/s];
$h_{air1,2}$ = Enthalpy of air at the inlet and outlet of dan [K];
W_{fan} = Required work for fan [kWe];
ρ_{air} = Density of air [kg/m^3];
W_{turb} = Work of turbine to surrounding [kWe];
Q_{hex} = Heat rate through the heat exchanger [kW_{th}];
Q_{vap} = Heat rate through the vaporizer [kW_{th}];
Q_{pre} = Heat rate through the preheater [kW_{th}];
CO_2 = Mass flow rate of produced CO_2 from power plant [kg/kWh];
$\dot{m}_{CO2}$ = Mass flow rate of produced CO_2 from gas power plant [kg/s];
W_{net} = Net power outlet of power plant [kWe].
η_{ORC} = Efficiency of ORC [%];
$\eta_{Power\ plant}$ = Overall efficiency of combined power plant [%].

REFERENCES

Ahmadi, A., Assad, M.E.H., Jamali, D.H., Kumar, R., Li, Z.X., Salameh, T., Al-Shabi, M. and Ehyaei, M.A., 2020: Applications of geothermal organic Rankine Cycle for electricity production. *Journal of Cleaner Production*, *274*, 122950.

Alboiu, V. and Walker, T.R., 2019: Pollution, management, and mitigation of idle and orphaned oil and gas wells in Alberta, Canada. *Environmental monitoring and assessment*, *191*(10), 1-16.

Alimonti, C., Soldo, E., Scrocca, D., 2021: Looking forward to a decarbonized era: geothermal potential assessment for oil & gas fields in Italy. *Geothermics, 93*, 102070.

Arabkoohsar, A. and Nami, H., 2019: Thermodynamic and economic analyses of a hybrid waste-driven CHP–ORC plant with exhaust heat recovery. *Energy Conversion and Management*, *187*, 512-522.

Augustine, C. and Falkenstern, D., 2014: An estimate of the near-term electricity-generation potential of coproduced water from active oil and gas wells. *SPE Journal*, *19*(03), 530-541.

Bachu, S., 2017: Analysis of gas leakage occurrence along wells in Alberta, Canada, from a GHG perspective–Gas migration outside well casing. *Int. J. Greenh. gas Control*, *61*, 146–154.

Boothroyd, I.M., Almond, S., Qassim, S.M., Worrall, F., Davies, R.J., 2016: Fugitive emissions of methane from abandoned, decommissioned oil and gas wells. *Sci. Total Environ.*, *547*, 461-469.

Braimakis, K., Charalampidis, A. and Karellas, S., 2021: Techno-economic assessment of a small-scale biomass ORC-CHP for district heating. *Energy Conversion and Management, 247,* 114705.

Breeze, P., 2018: *Combined heat and power*. Academic Press, London, United Kingdom, 95 pp.

Burnett, D.B., 2004: Potential for beneficial use of oil and gas produced water. *Global. Pet. Institute, Texas Water Resources Institute*, 1-11.

Chandhana, G.S., Kaveri, B.L. and Yuvaraja, T., 2018: Analysis of energy system in oil and gas industry. *Journal of Computational and Theoretical Nanoscience*, *15*(6-7), 2158-2160.

Chiasson, A.D., 2016: *Geothermal heat pump and heat engine systems: Theory and practice*. John Wiley & Sons, Chichester, UK, 472 pp.

Clauser, C., and Ewert, M., 2018: The renewables cost challenge: Levelized cost of geothermal electric energy compared to other sources of primary energy–Review and case study. *Renewable and Sustainable Energy Reviews, 82,* 3683-3693.

Curtice, R.J. and Dalrymple, E.D., 2004: Just the cost of doing business? *World oil*, *225*(10), 77-78.

Danesh, A., 1998: *PVT and phase behaviour of petroleum reservoir fluids*. Elsevier, 387 pp.

DiPippo, R., 2015: Geothermal power plants: Evolution and performance assessments. *Geothermics, 53,* 291-307.

Echchelh, A., Hess, T., and Sakrabani, R., 2018: Reusing oil and gas produced water for irrigation of food crops in drylands. *Agric. Water Manag., 206,* 124-134.

Erdlac Jr, R.J., Armour, L., Lee, R., Snyder, S., Sorensen, M., Matteucci, M. and Horton, J., 2007: Ongoing resource assessment of geothermal energy from sedimentary basins in Texas. *Proceedings of Thirty-second Workshop on Geothermal Reservoir Engineering, Stanford University, Stanford, California, US,* 8 pp.

Estrada, J.M., and Bhamidimarri, R., 2016: A review of the issues and treatment options for wastewater from shale gas extraction by hydraulic fracturing. *Fuel, 182,* 292-303.

Gehringer, M., and Loksha, V., 2012: *Handbook on planning and financing geothermal power generation*. ESMAP (Energy Sector Management Assistance Program), Main Findings and recommandations. The International Bank for Reconstruction and Developement, Washington.

Gosnold, W., 2017: *Electric power generation from low to intermediate temperature resources executive*. Univ. of North Dakota, Grand Forks, ND, USA, Technical Report.

Guerra, K., Dahm, K., and Dundorf, S., 2011: *Oil and gas produced water management and beneficial use in the Western United States.* US Department of the Interior, Bureau of Reclamation, 113 pp.

Haghighi, A., Pakatchian, M.R., Assad, M.E.H., Duy, V.N. and Alhuyi Nazari, M., 2020: A review on geothermal Organic Rankine cycles: modeling and optimization. *Journal of Thermal Analysis and Calorimetry*, *144*(5), 1799-1814.

Healy, R.W., Alley, W.M., Engle, M.A., McMahon, P.B., and Bales, J.D., 2015: The water-energy nexus an earth science perspective. *US geological survey circular,* 1407 pp + 107 pp.

Hu, K., Zhu, J., Zhang, W. and Lu, X., 2017: A case study of an ORC geothermal power demonstration system under partial load conditions in Huabei Oilfield, China. *Energy procedia*, *142*, 1327-1332.

Huttrer, G.W., 2020: Geothermal power generation in the world 2015-2020 update report. *Proceedings of the World Geothermal Congress 2020, Reykjavik, Iceland,* 17 pp.

Jackson, R.B., Vengosh, A., Darrah, T.H., Warner, N.R., Down, A., Poreda, R.J., Osborn, S.G., Zhao, K., and Karr, J.D., 2013: Increased stray gas abundance in a subset of drinking water wells near Marcellus shale gas extraction. *Proceedings of the National Academy of Sciences*, *110(28),* 11250-11255.

Javadi, M.H., Ebrahimi, D., and Nouraliee, J., 2020: *Feasibility study of harnessing geothermal energy in oil and gas fields*. Niroo Research Institute (NRI), Tehran, report in Persian.

Kang, M., Christian, S., Celia, M.A., Mauzerall, D.L., Bill, M., Miller, A.R., Chen, Y., Conrad, M.E., Darrah, T.H. and Jackson, R.B., 2016: Identification and characterization of high methane-emitting abandoned oil and gas wells. *Proceedings of the National Academy of Sciences*, *113(48),* 13636-13641.

Kang, M., Mauzerall, D.L., Ma, D.Z., and Celia, M.A., 2019: Reducing methane emissions from abandoned oil and gas wells: Strategies and costs. *Energy Policy, 132,* 594–601.

Kaplanoğlu, M.A., Baba, A., and Akkurt, G.G., 2020: Use of abandoned oil wells in geothermal systems in Turkey. *Geomechanics and Geophysics for Geo-Energy and Geo-Resources, 6,* 1-10.

Khatib, Z., and Verbeek, P., 2003: Water to value-produced water management for sustainable field development of mature and green fields. *J. Pet. Technol., 55,* 26-28.

Lee, K., & Neff, J. (eds.), 2011: *Produced water: environmental risks and advances in mitigation technologies*. Springer New York, NY, US, 608 pp.

Li, K., Bian, H., Liu, C., Zhang, D., and Yang, Y., 2015: Comparison of geothermal with solar and wind power generation systems. *Renew. Sustain. Energy Rev., 42,* 1464-1474.

Li, T., Zhu, J., and Zhang, W., 2012: Cascade utilization of low temperature geothermal water in oilfield combined power generation, gathering heat tracing and oil recovery. *Appl. Therm. Eng., 40,* 27-35.

Liu, C., Chen, P. and Li, K., 2014: A 500 W low-temperature thermoelectric generator: Design and experimental study. *International journal of hydrogen energy*, *39(28),* 15497-15505.

Liu, X., Falcone, G., and Alimonti, C., 2018: A systematic study of harnessing low-temperature geothermal energy from oil and gas reservoirs. *Energy, 142,* 346-355.

Liu, X., Gluesenkamp, K., and Momen, A., 2015: *Overview of available low-temperature / coproduced geothermal resources in the United States and the state of the art in utilizing geothermal resources for space conditioning in commercial buildings.* OAK Ridge National Laboratory, 18 pp.

Lund, J.W., 2000: World status of geothermal energy use overview 1995-1999. *Proceedings of the World Geothermal Congress 2000, Kyushu-Tohoku, Japan*, 4105-4111.

Lund, J.W., and Boyd, T.L., 2016: Direct utilization of geothermal energy 2015 worldwide review. *Geothermics, 60,* 66-93.

Lund, J.W., and Toth, A.N., 2021: Direct utilization of geothermal energy 2020 worldwide review. *Geothermics, 90,* 101915.

Macchi, E., 2017: Theoretical basis of the organic Rankine Cycle. In Macchi, E. and Astolfi, M. (eds.), *Organic Rankine Cycle (ORC) Power Systems*. Woodhead Publishing, 679 pp.

Matuszewska, D. and Olczak, P., 2020: Evaluation of using gas turbine to increase efficiency of the Organic Rankine Cycle (ORC). *Energies, 13(6),* 1499.

McMahon, P.B., Thomas, J.C., Crawford, J.T., Dornblaser, M.M., and Hunt, A.G., 2018: Methane in groundwater from a leaking gas well, Piceance Basin, Colorado, USA. *Sci. Total Environ., 634,* 791–801.

Moya, D., Aldás, C., and Kaparaju, P., 2018: Geothermal energy: Power plant technology and direct heat applications. Renew. *Sustain. Energy Rev., 94,* 889-901.

Nami, H., Ertesvåg, I.S., Agromayor, R., Riboldi, L. and Nord, L.O., 2018: Gas turbine exhaust gas heat recovery by organic Rankine cycles (ORC) for offshore combined heat and power applications-Energy and exergy analysis. *Energy, 165,* 1060-1071.

Nasiri, M., Jafari, I., and Parniankhoy, B., 2017: Oil and gas produced water management: a review of treatment technologies, challenges, and opportunities. *Chem. Eng. Commun., 204,* 990-1005.

Nian, Y.L., and Cheng, W.L., 2018: Insights into geothermal utilization of abandoned oil and gas wells. *Renew. Sustain. Energy Rev., 87*, 44-60.

Nordquist, J., and Johnson, L., 2012: Production of power from the co-produced water of oil wells, 3.5 years of operation. *Geothermal Resources Council, Transactions, 36,* 207-210.

Pathirathna, K.A.B., 2013: *Gas turbine thermodynamic and performance analysis methods using available catalog data.* University of Gavle, Sweden, Master thesis, 101 pp.

Ramirez, P., 2010: Bird mortality in oil field wastewater disposal facilities. *Environ. Manage., 46,* 820–826.

Sedlacko, E.M., Jahn, C.E., Heuberger, A.L., Sindt, N.M., Miller, H.M., Borch, T., Blaine, A.C., Cath, T.Y., and Higgins, C.P., 2019: Potential for beneficial reuse of oil and gas–derived produced water in agriculture: physiological and morphological responses in spring wheat (Triticum aestivum). *Environ. Toxicol. Chem., 38,* 1756–1769.

Sirivedhin, T., McCue, J., and Dallbauman, L., 2004: Reclaiming produced water for beneficial use: salt removal by electrodialysis. *J. Memb. Sci., 243,* 335–343.

Sivalls, C.R., 1987: *Oil and gas separation design manual*. Sivalls Incorporated.

Skalak, K.J., Engle, M.A., Rowan, E.L., Jolly, G.D., Conko, K.M., Benthem, A.J., and Kraemer, T.F., 2014: Surface disposal of produced waters in western and southwestern Pennsylvania: Potential for accumulation of alkali-earth elements in sediments. *Int. J. Coal Geol., 126*, 162–170.

Soltani, M., Moradi Kashkooli, F., Dehghani-Sanij, A.R., Nokhosteen, A., Ahmadi-Joughi, A., Gharali, K., Mahbaz, S.B., and Dusseault, M.B., 2019: A comprehensive review of geothermal energy evolution and development. *Int. J. Green Energy, 16,* 971–1009.

Tartière, T. and Astolfi, M., 2017: A world overview of the organic Rankine cycle market. *Energy Procedia, 129,* 2-9.

Tester, J.W., Anderson, B.J., Batchelor, A.S., Blackwell, D.D., DiPippo, R., Drake, E.M., Garnish, J., Livesay, B., Moore, M.C., and Nichols, K., 2006: The future of geothermal energy. *Massachusetts Inst. Technol, 358,* 13 pp.

Townsend-Small, A., Ferrara, T.W., Lyon, D.R., Fries, A.E., and Lamb, B.K., 2016: Emissions of coalbed and natural gas methane from abandoned oil and gas wells in the United States. *Geophys. Res. Lett., 43,* 2283–2290.

Wang, K., Yuan, B., Ji, G. and Wu, X., 2018: A comprehensive review of geothermal energy extraction and utilization in oilfields. *Journal of Petroleum Science and Engineering*, *168*, 465-477.

Wang, S., Yan, J., Li, F., Hu, J., and Li, K., 2016: Exploitation and utilization of oilfield geothermal resources in China. *Energies, 9,* 798.

Watson, S., Falcone, G., and Westaway, R., 2020: Repurposing hydrocarbon wells for geothermal use in the UK: the onshore fields with the greatest potential. *Energies, 13,* 3541.

Xin, S., Liang, H., Hu, B., and Li, K., 2012: A 400 kW geothermal power generator using co-produced fluids from Huabei oilfield. *Geotherm. Resour. Counc. Trans., 36,* 219-223.

Yang, Y., Huo, Y., Xia, W., Wang, X., Zhao, P., and Dai, Y., 2017: Construction and preliminary test of a geothermal ORC system using geothermal resource from abandoned oil wells in the Huabei oilfield of China. *Energy, 140,* 633-645.

Zhang, L., and Hascakir, B., 2021: A review of issues, characteristics, and management for wastewater due to hydraulic fracturing in the US. *J. Pet. Sci. Eng.,202,* 108536.

Zhang, Q., Zhang, H., Yan, Y., Yan, J., He, J., Li, Z., Shang, W., and Liang, Y., 2021: Sustainable and clean oilfield development: How access to wind power can make offshore platforms more sustainable with production stability. *J. Clean. Prod., 294,* 126225.

APPENDIX

The appendix of this report presents in detail the thermodynamic characteristics of each case in the form of a diagram.

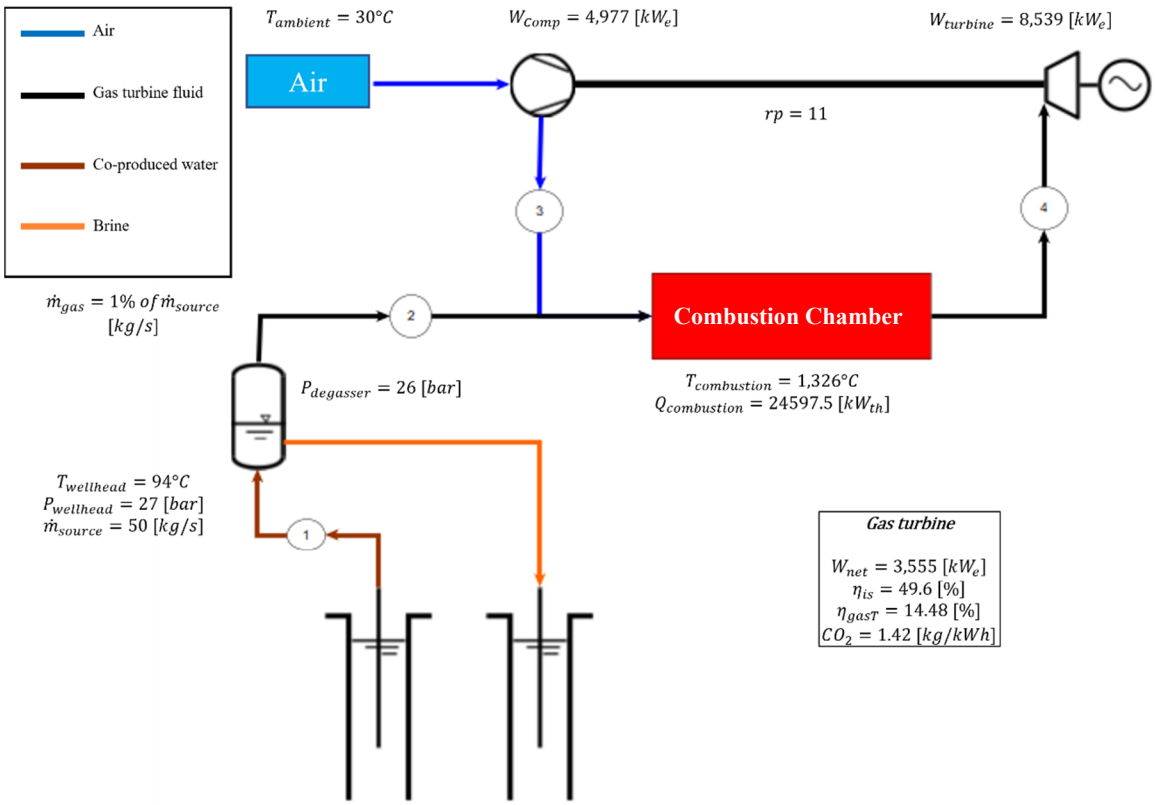

FIGURE A1: Thermodynamic diagram of case 1 (only gas turbine)

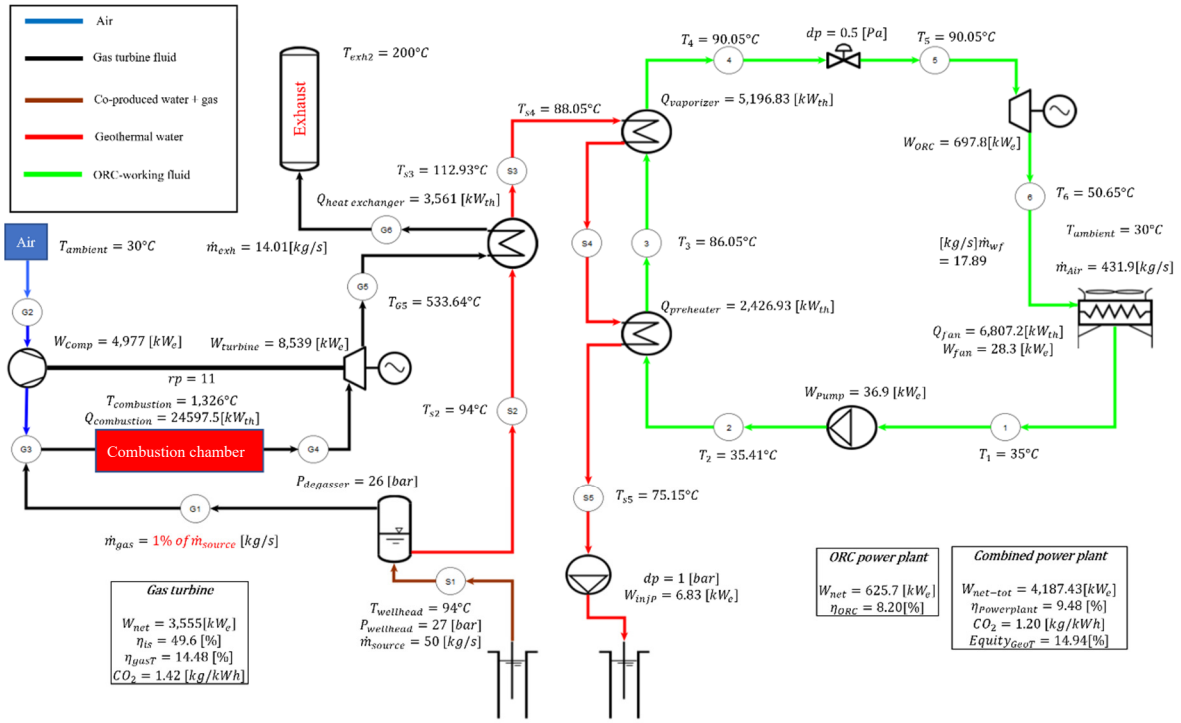

FIGURE A2: Thermodynamic diagram of case 2 (combined system)

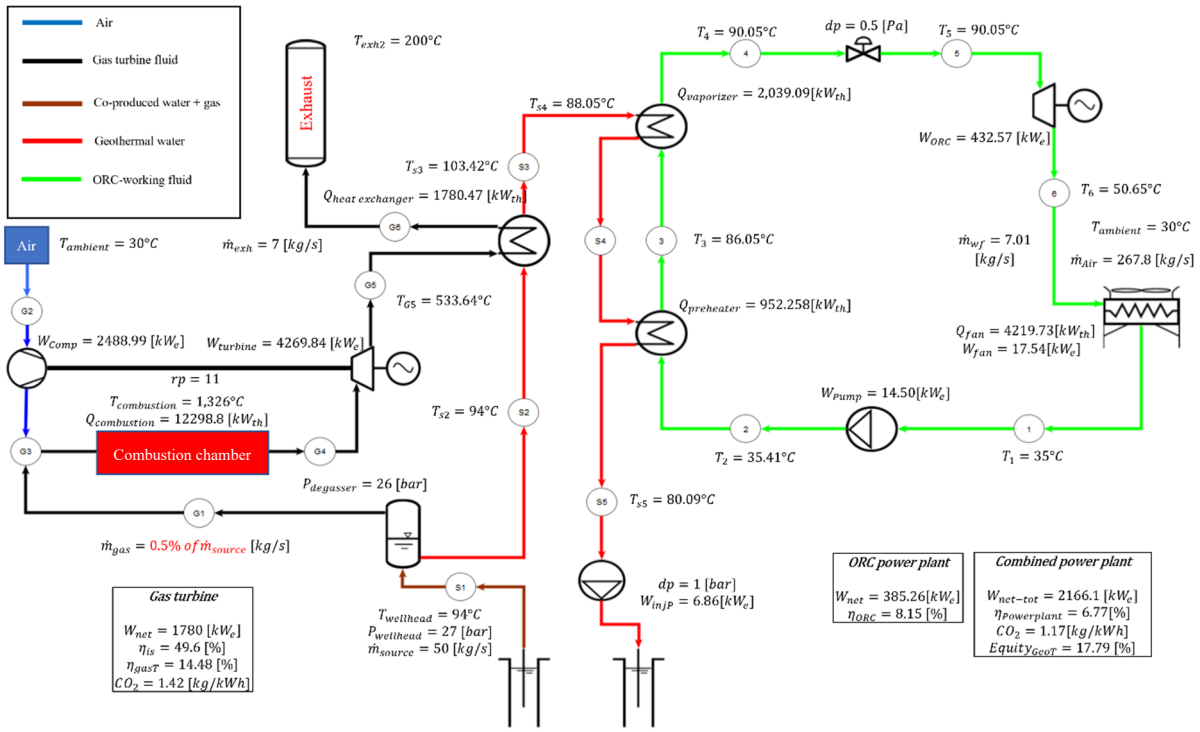

FIGURE A3: Thermodynamic diagram of case 3 (combined system)